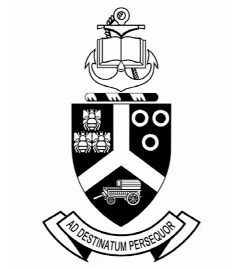


# Iterative Solution of the Dirac Equation using the Lanczos Algorithm



Richard Andrew

Faculty of Natural & Agricultural Science

University of Pretoria

Pretoria

Submitted in partial fulfilment of the requirements for the degree

*Magister Scientae*

20th May 2008

## Acknowledgements

And I would like to acknowledge the following:

- Prof. H. Miller for his help and guidance
- The National Research Foundation for their financial support

## Summary

The Lanczos algorithm (Lanczos (1950)) is an efficient method for obtaining the eigenpairs of large hermitian matrices and/or self-adjoint operators. This present work considers the latter case where the algorithm uses a bounded operator and a suitably chosen start function to construct and tri-diagonalize a matrix representation of the operator in an iterative manner and find its absolutely convergent eigensolutions (Parlett (1980)).

The relativistic Dirac Hamiltonian operator, which describes an electron in an external central field, has the added complication of two sets of continua and a point spectrum; one set of continua for positive energy solutions and the other for negative energies with the point spectrum bounded above and below. It is this combination which form a complete basis for the Dirac Hamiltonian. This has led to the development of non-physical spurious solutions in many solution methods (Andrew and Miller (2007)). The same problem occurs in the Lanczos algorithm (Lanczos (1950)) when it is applied to operators which possess bound state spectra as well as continua (Andrew and Miller (2003)) such as the Dirac Problem.

It is proposed that exact eigenpairs can be identified in the following manner (Andrew and Miller (2003)). After each iteration, for each of the converging eigenpairs  $(e_{l\lambda}, |e_{l\lambda}\rangle)$ ,  $\Delta_{l\lambda} = |e_{l\lambda}^2 - \langle e_{l\lambda} | \hat{H}^2 | e_{l\lambda} \rangle|$  (where  $l$  is the iteration number) is calculated and a determination is made as to whether  $\Delta$  is converging toward zero or not. In other words, one could check to see whether the eigensolutions from the diagonalisation of the projected operator  $(\hat{H}_P)$  are also eigensolutions of  $\hat{H}^2$ . For the exact bound states of  $\hat{H}$ ,  $\Delta$  must be precisely zero and the other eigenstates states of  $\hat{H}_P$  should converge to some non-zero positive value. This method has been successfully implemented to identify spurious states in non-relativistic Quantum Mechanics (Andrew and Miller (2003)).

These methods are applied to the Dirac problem in this thesis to solve the ground state eigenpairs for the Coulomb and Yukawa potentials.

# Contents

<b>1</b>	<b>Introduction</b>	<b>1</b>
<b>2</b>	<b>Application of the Lanczos Method to Self-Adjoint Operators</b>	<b>5</b>
2.1	Introduction . . . . .	5
2.2	The Lanczos Method . . . . .	6
2.3	Identifying spurious solutions . . . . .	7
2.4	Application to a Hamiltonian Operator . . . . .	8
2.4.1	Results for $a = \sqrt{2}$ . . . . .	9
2.4.2	Results for $a = 6$ . . . . .	11
2.4.3	Discussion . . . . .	14
<b>3</b>	<b>Dirac Theory</b>	<b>15</b>
3.1	Introduction . . . . .	15
3.2	Solutions to the Dirac Equation in a Central Potential . . . . .	16
3.3	The Dirac Eigen Equation . . . . .	17
<b>4</b>	<b>Numerical Results</b>	<b>19</b>
4.1	Dirac Equation for a Coulomb Potential . . . . .	19
4.1.1	Results: Coulomb Potential . . . . .	19
4.2	Dirac Equation for a Yukawa Potential . . . . .	22
4.2.1	Results: Yukawa Potential . . . . .	22
<b>5</b>	<b>Conclusions</b>	<b>25</b>
	<b>References</b>	<b>28</b>

# List of Figures

2.1	$\Delta_{\lambda n}$ and $e_{\lambda n}$ for $a = \sqrt{2}$ . . . . .	10
2.2	Ground State eigenvector for $a = \sqrt{2}$ . . . . .	11
2.3	$\Delta_{\lambda n}$ and $e_{\lambda n}$ for $a = 6$ . . . . .	12
2.4	Ground State eigenvector for $a = 6$ . . . . .	13
4.1	Plot of $e_{\lambda n}$ convergence for Coulomb bound state and spurious solution for $\gamma = 1.01$ . . . . .	20
4.2	Plot of $\Delta_{\lambda, n}$ convergence for Coulomb bound state and spurious solution for $\gamma = 1.01$ . . . . .	21
4.3	Plot of $e_{\lambda n}$ convergence for Yukawa bound state and spurious solution for $\gamma = 1.001$ . . . . .	23
4.4	Plot of $\Delta_{\lambda, n}$ convergence for Yukawa bound state and spurious solution for $\gamma = 1.001$ . . . . .	24

# Nomenclature

## Notes

Please note that the numbers behind each reference in the References section refer to the page number on which the particular reference is found.

# Chapter 1

## Introduction

The relativistic Dirac Hamiltonian operator, which describes an electron in an external central coulomb-like field, has the added complication of two sets of continua and a point spectrum; one set of continua for positive energy solutions and one set for negative energies with the point spectrums bounded above and below. It is this combination which form a complete basis for the Dirac Hamiltonian. Recently, much effort has focused on the extension of basis set methods (Drake and Goldman (1981); Goldman and Drake (1982, 1988); Krauthauser and Hill (2002)) applied with success in non-relativistic Quantum Mechanics. Such matrix approximations of the Dirac equation are usually obtained from a variational principle with the radial components of the spinor-wave function approximated by a finite number of terms of a basis-set expansion. These methods often display pathological features such as the occurrence of unphysical spurious solutions (Kutzelnigg (1984), Andrew and Miller (2007)) since the basis-sets do not form a complete basis and fail to vary systematically with the basis-set size. Although these problems can for the most part be avoided if a resolvent operator rather than the Dirac Hamiltonian is used in the variational principle (Krauthauser and Hill (2002)) or by construction in explicit finite basis-set calculations (Goldman (1985)), the convergence of these methods depend on the size of the basis set.

Recently Ackad and Horbatsch (Ackad and Horbatsch (2005)) have presented an elegant numerical method for the solution of the Dirac equation using the Rayleigh-Ritz method (Krauthauser and Hill (2002)). Using a mapped Fourier grid method, a matrix representation of the Dirac Hamiltonian is constructed



in a Fourier-sine basis which, upon diagonalisation yields reasonably numerically accurate eigenvalues for a mesh size which is not exceptionally large. Relativistic sum rules (Goldman and Drake (1982)) provide a simple means of checking whether or not the number of basis states is adequate. As with any attempt to construct a matrix representation of an operator which contains continuum states, spurious states can occur and must be eliminated. Ackad and Horbatsch (Ackad and Horbatsch (2005)) have pointed out that in certain cases they can be identified by looking at the numerical structure of the large and small components of the corresponding eigenvector. They also point out that similar phenomena occur in the Fourier grid representation of the non-relativistic Schrödinger problem (Willner et al. (2004)) in which non-physical roots are observed at random locations.

The genesis of these spurious states can easily be understood, and there is a simple way to identify them. Consider an operator,  $\hat{H}$ , which possess a continuum (or continua) as well as a point spectrum. The subspace spanned by its bound state eigenfunctions,  $\mathcal{H}_B$ , is by itself incomplete. As the composition of this space is generally not known beforehand, a set of basis states which is complete and spans a space,  $\mathcal{F}$ , is chosen to construct a matrix representation of the operator,  $\hat{H}$ , to be diagonalized. Mathematically, this corresponds to projecting the operator  $\hat{H}$  onto the space  $\mathcal{F}$ . Clearly the eigenpairs obtained from diagonalizing the projected operator,  $\hat{H}_P$ , need not all be the same as those of the operator  $\hat{H}$ . However, because the set of basis states is complete, any state contained in  $\mathcal{H}_B$  can be expanded in terms of this set of basis states. Hence  $\mathcal{H}_B$  may also be regarded as a subspace of  $\mathcal{F}$  and the complete diagonalization of  $\hat{H}_P$  will yield not only the exact eigenstates of  $\hat{H}$  but additional spurious eigensolutions. Note that these spurious eigenfunctions are eigenfunctions of  $\hat{H}_P$  and not of  $\hat{H}$ . Furthermore, in this case the Rayleigh-Ritz bounds discussed in the paper by Krauthauser and Hill (Krauthauser and Hill (2002)) apply to the eigenstates of  $\hat{H}_P$ .

It is interesting to note that the same problem occurs in the Lanczos algorithm (Lanczos (1950)) when it is applied to operators which possess a bound state spectrum as well as a continuum (Andrew and Miller (2003)). This is not surprising as the Lanczos algorithm can also be considered as an application

of the Rayleigh-Ritz method (Parlett (1980)). In this case an orthonormalized set of Krylov basis vectors is used to iteratively construct a matrix representation of the operator which is then diagonalized. Again, spurious states can occur for precisely the same reasons as stated previously. In this case it is proposed to identify the exact bound states in the following manner (Andrew and Miller (2003)). After each iteration, for each of the converging eigenpairs  $(e_{l\lambda}, |e_{l\lambda}\rangle)$ ,  $\Delta_{l\lambda} = |e_{l\lambda}^2 - \langle e_{l\lambda} | \hat{H}^2 | e_{l\lambda} \rangle|$  (where  $l$  is the iteration number) is calculated and a determination is made as to whether  $\Delta$  is converging toward zero or not. Alternatively, one could check to see whether the eigensolutions from the diagonalization of the projected operator  $(\hat{H}_P)$  are also eigensolutions of  $\hat{H}^2$ . For the exact bound states of  $\hat{H}$ ,  $\Delta$  must be precisely zero while the other eigenstates states of  $\hat{H}_P$  should converge to some non-zero positive value. This method has been successfully implemented to identify spurious states in non-relativistic (Andrew and Miller (2003)) eigenvalue problems. A similar procedure can be implemented in any Rayleigh-Ritz application.

In this dissertation, the Lanczos method will be applied to obtain approximate eigensolutions of the Dirac operator for a relativistic electron in a central potential. The advantages of using the Lanczos method to solve the Dirac problem are:

1. It can be applied to any self-adjoint operator which possesses at least one bound and is an absolutely convergent method.
2. The lowest-lying eigenpairs usually converge the quickest (Parlett (1980)), and one is able to obtain good approximations to the lowest-lying eigenpairs in this manner (especially the ground state).
3. The identification and removal of any spurious state solutions can easily be implemented (Andrew and Miller (2003), Andrew et al. (2007)).

This dissertation is structured as follows:  
Chapter 2 describes the Lanczos algorithm as it applies to bounded hermitian operators and describes a method for identifying spurious solutions. An application of a 1-D Schrödinger equation problem is given as an example.

Chapter 3 presents the Dirac problem for a relativistic electron in a central potential.

Chapter 4 presents the numerical results for solving the Dirac problem for a hydrogen like atom using the Coulomb and Yukawa potentials.

## Chapter 2

# Application of the Lanczos Method to Self-Adjoint Operators

### 2.1 Introduction

There is a growing interest in using numerical methods such as the Lanczos Algorithm (Lanczos (1950) , Andrew and Miller (2003), Miller (1994)) to solve Quantum Mechanical problems. Given a suitable start vector  $|T\rangle$  and provided the operator has either an upper or a lower bound, the Lanczos algorithm is an absolutely convergent algorithm which yields approximate eigenvalues and eigenvectors of  $\hat{H}$  after a suitable number of iterations (Kreuzer et al. (1981a)).

The problem for the Quantum Mechanical self-adjoint operator  $\hat{H}$  (fully as well as semi-bounded), is to find a suitable trial vector that also satisfies the boundary conditions of the wave equation. If the bound states formed a complete basis set,  $|T\rangle = \sum_n a_n |E_n\rangle$  where  $|E_n\rangle$  are the exact bound states of  $\hat{H}$  would be the best choice since the algorithm would yield only for the bound states. Since they do not form a complete set if  $\hat{H}$  contains a continuous spectrum,  $|T\rangle$  is chosen from a complete set of analytic  $\mathcal{L}^2$  functions which define a space  $\mathcal{F}$ . When the Lanczos algorithm is applied to  $|T\rangle$ , the eigenpairs obtained will correspond to those of the operator  $\hat{H}$  projected onto  $\mathcal{F}$ . A subset of these eigenpairs must

## 2.2 The Lanczos Method

---

correspond to the exact eigenpairs of the unprojected Hamiltonian operator since the exact eigenstates can be expanded in terms of the complete set of states which span  $\mathcal{F}$ . The remaining subset of eigenpairs contain spurious solutions of the projected Hamiltonian. It only remains to identify the exact eigenpairs even if they are not completely converged.

## 2.2 The Lanczos Method

Given the following eigenvalue problem

$$\hat{H}|E_\lambda\rangle = E_\lambda|E_\lambda\rangle \quad (2.1)$$

where  $\hat{H}$  is a self-adjoint operator (not necessarily bounded) in a separable Hilbert (or Sobolev) space which possesses a number of eigenvalues  $E_\lambda$  (not necessarily bounded from above) which ascend from a minimal one  $E_1$ . Furthermore let  $|1\rangle$  be a normalised start vector having the properties that:

1.  $\hat{H}^k|1\rangle$  exists for all non-negative integers  $k$  and
2.  $\langle x|1\rangle$  satisfies the boundary conditions.

The algorithm may then be stated as follows. Calculate successively the vectors

$$|\phi_1\rangle := |1\rangle \quad (2.2)$$

$$|\phi_{n+1}\rangle := \frac{1}{\|\dots\|}(\hat{H}^n|1\rangle - \sum_{n'=1}^n |\phi_{n'}\rangle\langle\phi_{n'}|\hat{H}^n|1\rangle), \quad n = 1, 2, 3, \dots \quad (2.3)$$

where  $n$  is the iteration number. The Lanczos Method solves the eigenproblem by diagonalizing successively the operators

$$\hat{H}_n := \sum_{m,m'=1}^n |\phi_m\rangle\langle\phi_m|\hat{H}|\phi_{m'}\rangle\langle\phi_{m'}|. \quad n = 1, 2, 3, \dots \quad (2.4)$$

The orthonormalized Lanczos vectors  $|\phi_n\rangle$  fulfil the following recursion relations (Kreuzer et al. (1981a)):

$$|\phi_n\rangle = p_n(\hat{H})|1\rangle \quad (2.5)$$

## 2.3 Identifying spurious solutions

---

where the Lanczos polynomials  $p_n(x)$  are defined in the following way:

$$p_1(x) := 1 \quad p_2(x) := w_1^{-1}(x - v_1), \quad (2.6)$$

$$p_{n+1}(x) := w_n^{-1}[(x - v_n)p_n(x) - w_{n-1}p_{n-1}(x)] \quad n = 2, 3, 4, \dots, \quad (2.7)$$

with

$$v_n := \langle \phi_n | \hat{H} | \phi_n \rangle \quad (2.8)$$

$$w_n := \langle \phi_{n+1} | \hat{H} | \phi_n \rangle. \quad (2.9)$$

Performing the diagonalizations in equation 2.4 reduces to finding the roots of the following characteristic polynomial:

$$\det(\hat{H}_n - x \cdot \hat{1}) := (-1)^n w_1 \dots w_n p_{n+1}(x) \quad (2.10)$$

after each iteration step.

Eigenvectors are constructed from the Lanczos vectors using

$$|e_{\lambda n}\rangle = \frac{1}{\|\dots\|} \sum_{n'=1}^n p_{n'}(e_{\lambda n}) |\phi_{n'}\rangle \quad (2.11)$$

after each iteration step.

The generated sequence of eigenpairs  $(e_{\lambda n}, |e_{\lambda n}\rangle)$  possess the following convergence properties (Kreuzer et al. (1981a)):

$$e_{\lambda n} \xrightarrow[n \rightarrow \infty]{} E_{\lambda}, \quad \lambda = 1, 2, 3, \dots, \quad (2.12)$$

$$|e_{\lambda n}\rangle \xrightarrow[n \rightarrow \infty]{} |E_{\lambda}\rangle, \quad \lambda = 1, 2, 3, \dots \quad (2.13)$$

For a self-adjoint operator the Lanczos algorithm can be implemented using *Mathematica* (Wolfram (1991)).

## 2.3 Identifying spurious solutions

For those operators which possess a continuum as well as a point spectrum, the space spanned by the bound state eigenvectors is by itself certainly not complete

## 2.4 Application to a Hamiltonian Operator

---

and a suitable start vector should be composed only of components in the subspace spanned by the bound state eigenvectors. The exact bound states can be identified in the following manner (Andrew and Miller (2003)). Usually the start vector is chosen from a complete set of analytic functions which define a space  $\mathcal{F}$ . This space is in most cases not necessarily of the same dimension as the subspace spanned by the exact eigenvectors. On the other hand, if the Lanczos algorithm is applied with this choice for the start vector, the eigenpairs obtained will correspond to those of the operator projected onto  $\mathcal{F}$ . A subset of these eigenstates must correspond to the exact eigenpairs of the unprojected Hamiltonian operator since the exact eigenstates can be expanded in terms of the complete set of states which span  $\mathcal{F}$ . After each iteration, for each of the converging eigenpairs  $(e_{\lambda_n}, |e_{\lambda_n}\rangle)$ ,  $\Delta_{\lambda_n} = |e_{\lambda_n}^2 - \langle e_{\lambda_n} | \hat{H}^2 | e_{\lambda_n} \rangle|$  (where  $n$  is the iteration number) is calculated and a determination is made as to whether  $\Delta$  is converging toward zero or not. For the exact bound states of  $\hat{H}$ ,  $\Delta$  must be precisely zero, while the other eigenstates states of the projected operator should converge to some non-zero positive value. Provided sufficient iterations are performed, it should be possible to identify uniquely the approximate eigenpairs in this manner which ultimately will converge to the exact bound states. Since in the the Lanczos algorithm the lowest-lying eigenpairs (for an operator which possesses at most a lower bound) usually converge the fastest (Parlett (1980)), one should be able to obtain good approximations to the lowest-lying eigenpairs.

## 2.4 Application to a Hamiltonian Operator

To numerically verify this, the algorithm was applied to a one dimensional  $\hat{H}$  with an inverse Gaussian potential. The start wave function  $\langle x|T\rangle$  was a normalised Gaussian (since it satisfied the boundary conditions). The choice of potential only allowed for negative bound state energies and made their visual identification easy. Initially, the potential was chosen so that  $\hat{H}$  had only one even parity bound state, then the potential was chosen such that  $\hat{H}$  contained more than one even parity bound state.

## 2.4 Application to a Hamiltonian Operator

---

The Hamiltonian chosen had the form:

$$\hat{H} = -\frac{\partial^2}{\partial x^2} - \exp\left(-\left(\frac{x}{a}\right)^2\right) \quad (2.14)$$

The start wave function was chosen to satisfy the boundary conditions at  $\pm\infty$  such that  $\Phi(-\infty) = \Phi(\infty) = 0$ . The Gaussian start function used was:

$$\langle x|T\rangle = \Phi_1(b, x) = \left(\frac{2b}{\pi}\right)^{1/4} \exp(-bx^2) \quad (2.15)$$

This choice of wave function ( $\Phi(b, x) \rightarrow \Phi(b, |x|)$  for  $x < 0$ ) restricted solutions to even parity since parity is conserved. For this particular choice of start function:

$$\int_{-\infty}^{\infty} \Phi^*(b, x)x^n \exp(mx^2)\Phi(b, x)dx = \sqrt{\frac{1}{2\pi}}(1+(-1)^n)(2-m)^{-(1+n)/2}\Gamma((1+n)/2) \quad (2.16)$$

This simplified the calculations in the Lanczos algorithm and reduced the numerical error (Miller (1994)).

Two cases were considered with differing well parameters: one with  $a = \sqrt{2}$  which possesses one exact even parity bound state, and one with  $a = 6$  which possesses two exact even parity bound states. The parameter  $b$  was chosen to minimise  $\langle \Phi_1|\hat{H}|\Phi_1\rangle$  and was rounded up to the nearest integer in order to minimise numerical errors. For both cases  $b = 1$ . This parameter caused the Lanczos algorithm to start near zero for the first eigenvalue thus speeding up the convergence for the negative bound state eigenvalues.

### 2.4.1 Results for $a = \sqrt{2}$

The approximate energy value for the ground state was found using the zero order Sturmian approximation (Mostafazadeh (2001)). Its value was  $-0.467154$ . The Lanczos algorithm gave values of  $e_o = -0.47615849$  and  $e_1 = 0.50306464$  after 15 iterations where  $e_o$  is the bound state and  $e_1$  is the first spurious state.

Figure 2.1 shows the convergence of the  $e_{l\lambda}$  and  $\Delta_{l\lambda}$  values. Note that the  $\Delta$ 's converge in a similar manner to the eigenvalues and that the values for the ground state converge the fastest.



## 2.4 Application to a Hamiltonian Operator

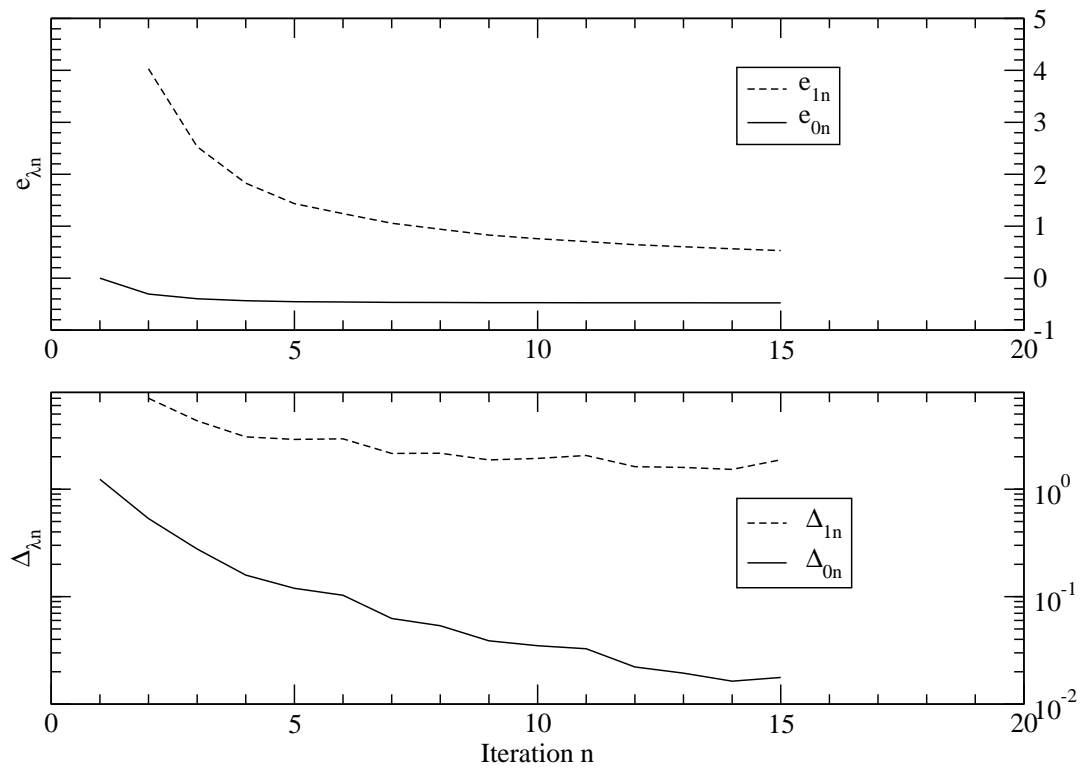


Figure 2.1:  $\Delta_{\lambda n}$  and  $e_{\lambda n}$  for  $a = \sqrt{2}$

## 2.4 Application to a Hamiltonian Operator

---

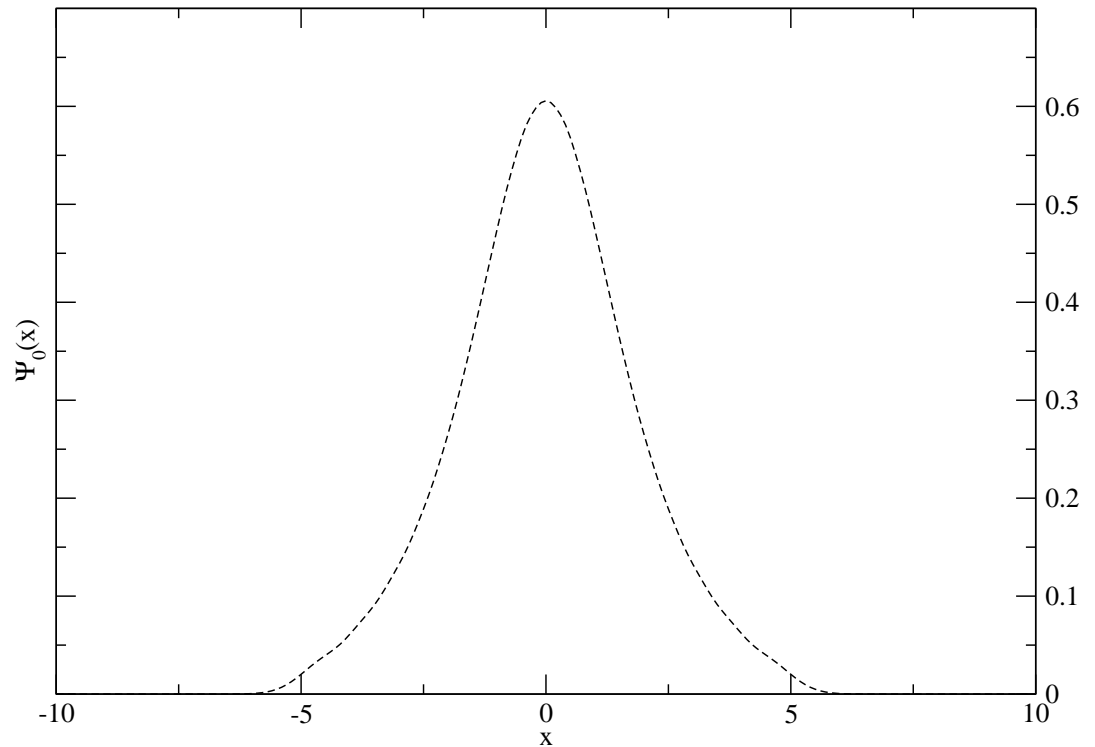


Figure 2.2: Ground State eigenvector for  $a = \sqrt{2}$

The results show that for iterations  $> 4$ , the ground state  $\Delta$  converges quickly to zero while the first non-bound state converges to a non-zero value. The eigenvector for the ground state is shown in Figure 2.2. It shows a symmetrical even parity wave function with a central anti-node at the origin.

### 2.4.2 Results for $a = 6$

The energy value for the ground state using the Sturmian approximation (Mostafazadeh (2001)) is  $e_o = -0.843599$ , while the Lanczos algorithm gave a value of  $-0.83781631$  after 15 iterations. The algorithm also found the next highest even bound state

## 2.4 Application to a Hamiltonian Operator

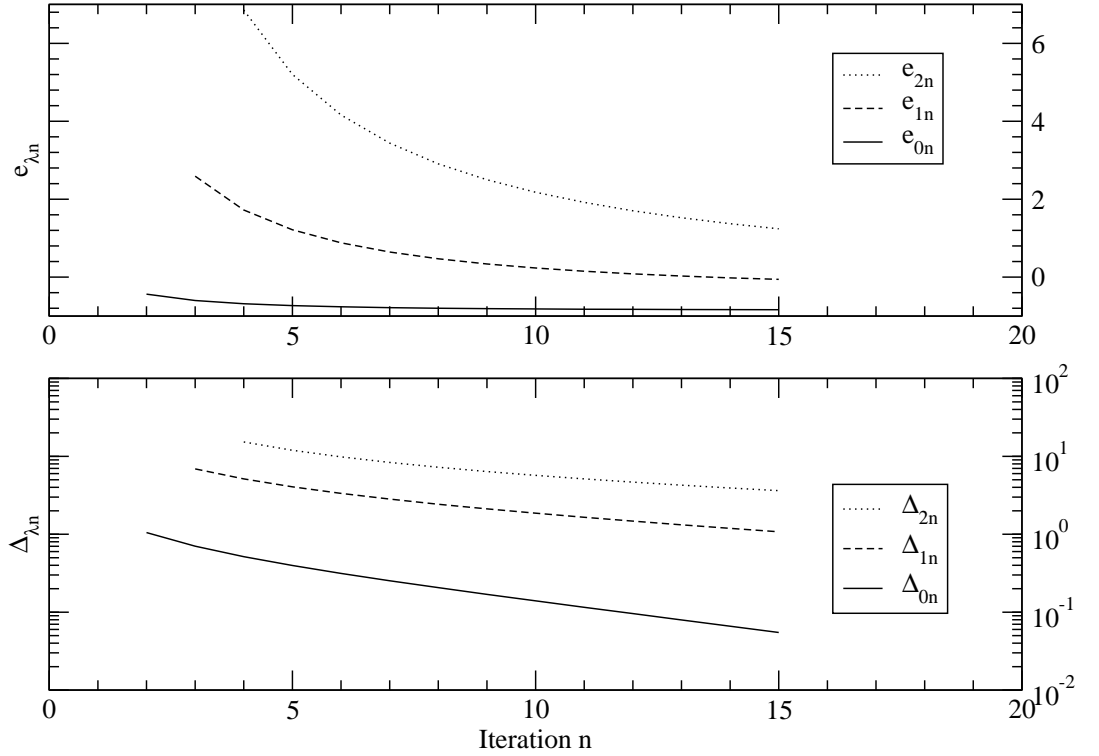


Figure 2.3:  $\Delta_{\lambda n}$  and  $e_{\lambda n}$  for  $a = 6$

$e_1$  which had a value of  $-0.09117731$ . The next spurious state had a value of  $e_2 = 1.12552398$  using the Lanczos Algorithm.

Figure 2.3 shows the convergence of the  $e_{l\lambda}$  and  $\Delta_{l\lambda}$  values. It shows that the  $\Delta$ 's converge in a similar manner to the eigenvalues and that the values for the ground state converge the fastest.  $\Delta$  for the bound states converges to zero while the non-bound state converges to a positive value. The eigenvector for the two bound states are shown in Figure 2.4. The ground state is similar to the  $a = \sqrt{2}$  case while the next even parity state has a central anti-node and two symmetrical side anti-nodes. These three anti-nodes signify it is the second bound state solution with even parity.

## 2.4 Application to a Hamiltonian Operator

---

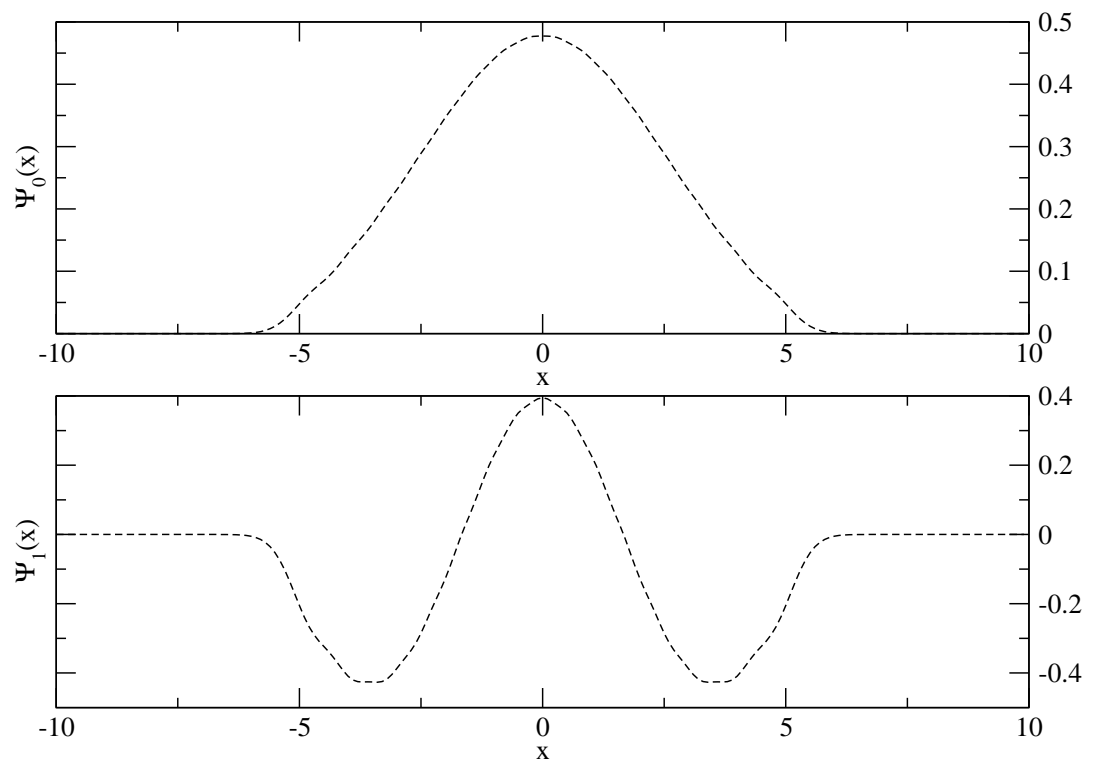


Figure 2.4: Ground State eigenvector for  $a = 6$

---

## 2.4 Application to a Hamiltonian Operator

### 2.4.3 Discussion

The numerical results show that for the bound states,  $\Delta$  converges to values approaching zero, while the non-bound states converge to positive constant values. The results also show that the ground state eigenvalue converges the fastest (Parlett (1980), Miller and Berger (1979)) which confirms that this method identifies the exact bound states of a given Hamiltonian. By applying the Lanczos algorithm to a reasonable choice for the start function after a suitable number of iterations, those eigenfunctions which have  $\Delta < \epsilon$  (for example,  $\epsilon = 1$ ) can be identified as the bound states.

# Chapter 3

## Dirac Theory

### 3.1 Introduction

The Dirac problem with a Coulomb potential coupling constant which is less than  $\frac{\sqrt{3}}{2}$  can be defined by a Hamiltonian that is self-adjoint in the first Sobolev space (Thaller (1992).) For this reason solutions of the Dirac Equation can be obtained in an absolutely convergent manner using the Lanczos Algorithm. Although this method is generally known for its application to conventional matrix-algebra eigenvalue problems (Lanczos (1950), it can be used to solve eigenvalue problems of a self-adjoint operator which is bounded from above or below (Kreuzer et al. (1981b).) In the former application, the matrix to be diagonalized is iteratively transformed into a tri-diagonal matrix and diagonalized after each iteration step to form a sequence of convergent eigenvalue solutions. In the operator application, a tri-diagonal representation of the self-adjoint operator is constructed iteratively and diagonalized after each iteration step to form a sequence of convergent eigenvalue solutions. Any spurious solutions which arise from the presence of continuum states can easily be identified by observing the iterative behaviour of a calculated parameter  $\Delta$  (Andrew and Miller (2003).) Furthermore as pointed out in the introduction, many of the aforementioned problems found in previous solution methods are avoided if the following iterative scheme proposed by Lanczos is employed.

Dirac theory requires that any relativistic particle with non-zero spin must satisfy the following requirements:

### 3.2 Solutions to the Dirac Equation in a Central Potential

---

- It must satisfy a first-order differential equation in all four relativistic coordinates.
- The equation must be linear to satisfy the superposition principle.
- The equation must satisfy the Klein-Gordon equation and in the classical limit, classical relativity.

Written in non-covariant form, the Dirac equation in an external electric field which satisfies the above requirements is:

$$E\Psi - V(r)\Psi = c\alpha \cdot \frac{\hbar}{i}\nabla\Psi + \beta mc^2\Psi \quad (3.1)$$

where  $\alpha$  and  $\beta$  are the  $4 \times 4$  hermitian Dirac matrices and  $\Psi$  is a four-component wave function with components  $u_1, u_2, u_3, u_4$ .

### 3.2 Solutions to the Dirac Equation in a Central Potential

Bethe provides a perturbative solution to this problem by first considering the case where the small components of  $\Psi$  ( $u_3$  and  $u_4$ ) are set to zero.  $u_1$  and  $u_2$  are set to the Pauli functions with the radially dependent parts set to arbitrary functions instead of the Schrödinger radial functions and making them eigenfunctions of the angular momentum quantum number  $l$  (Bethe (1964)). For  $j = l + 1/2$

$$u_1 = g(r)\sqrt{\frac{l+m+1/2}{2l+1}}Y_{l,m-1/2}(\Omega), \quad (3.2)$$

$$u_2 = -g(r)\sqrt{\frac{l-m+1/2}{2l+1}}Y_{l,m+1/2}(\Omega), \quad (3.3)$$

where  $Y_{l,m}(\Omega)$  are spherical harmonic functions. Since the small components share the same  $j$  value but must have a different  $l$ ,  $u_3$  and  $u_4$  are chosen as follows using suitable Clebch-Gordan coefficients:

$$u_3 = -if(r)\sqrt{\frac{l-m+3/2}{2l+3}}Y_{l+1,m-1/2}(\Omega), \quad (3.4)$$

### 3.3 The Dirac Eigen Equation

$$u4 = -if(r)\sqrt{\frac{l+m+3/2}{2l+3}}Y_{l+1,m+1/2}(\Omega). \quad (3.5)$$

Placing Equations 3.2, 3.3, 3.4 and 3.5 into Equation 3.1 and integrating over the solid angle  $\Omega$  yields the following coupled differential equations for the radial functions  $f(r)$  and  $g(r)$ :

$$-\hbar c \frac{df}{dr} - \frac{(1-\kappa)\hbar c}{r}f(r) = (E - V(r) - mc^2)g(r), \quad (3.6)$$

$$\hbar c \frac{dg}{dr} + \frac{(1+\kappa)\hbar c}{r}g(r) = (E - V(r) + mc^2)f(r), \quad (3.7)$$

where  $\kappa$  is a quantum number analogous to the angular momentum quantum number  $l$  in non-relativistic quantum mechanics.

Using  $F(r) = rf(r)$ ,  $G(r) = rg(r)$  and relativistic units  $\hbar = m_e = c = 1$  the equations become

$$-\frac{dF}{dr} + \frac{\kappa}{r}F(r) = (E - V(r) - 1)G(r), \quad (3.8)$$

$$\frac{dG}{dr} + \frac{\kappa}{r}G(r) = (E - V(r) + 1)F(r). \quad (3.9)$$

Using a power series expansion for  $G(r)$  and  $F(r)$ , Bethe was able to show that the bound state energies for a coulomb potential with charge  $z$  are given by:

$$e_{\kappa n} = \left(1 + \frac{(z\alpha)^2}{(n + \sqrt{\kappa^2 - (z\alpha)^2})^2}\right)^{-1} \quad (3.10)$$

for  $n = 0, 1, 2, 3, \dots$

### 3.3 The Dirac Eigen Equation

Equations (3.8) and (3.9) can be written in matrix notation

$$\begin{pmatrix} (V(r) + 1) & -\left(\frac{d}{dr} - \frac{\kappa}{r}\right) \\ \left(\frac{d}{dr} + \frac{\kappa}{r}\right) & (V(r) - 1) \end{pmatrix} \begin{pmatrix} G(r) \\ F(r) \end{pmatrix} = E \begin{pmatrix} G(r) \\ F(r) \end{pmatrix} \quad (3.11)$$

or simplify as

$$\hat{H}_D|\psi\rangle = E|\psi\rangle \quad (3.12)$$



### 3.3 The Dirac Eigen Equation

---

where

$$|\psi\rangle = \begin{pmatrix} G(r) \\ F(r) \end{pmatrix} \quad (3.13)$$

Equation (3.12) defines the eigenvalue problem which will be solved iteratively using the Lanczos algorithm.

## Chapter 4

# Numerical Results

### 4.1 Dirac Equation for a Coulomb Potential

To demonstrate that the the Lanczos algorithm may be used to solve the Dirac equation with a Coulomb potential:

$$V(r) = \frac{z\alpha}{r} \quad (4.1)$$

where  $\alpha$  is the fine structure constant, a start function was chosen using a slightly perturbed ground state solution derived by Bethe (Bethe (1964)) with  $\kappa = -1$  and  $z = 1$ . The exact ground state eigenvalue should equal  $s = \sqrt{1 - (z\alpha)^2}$ .

The start function contained the following perturbed radial functions

$$G_1(r) = (r^s)^\gamma e^{-z\alpha r} \quad (4.2)$$

$$F_1(r) = \frac{(s-1)(r^s)^\gamma e^{-z\alpha r}}{z\alpha} \quad (4.3)$$

where  $0 < \gamma < 1$  where  $\gamma$  is the perturbation factor. Note that this choice for the start function eliminates the possibility of obtaining negative energy eigen-solutions (Bethe (1964)).

#### 4.1.1 Results: Coulomb Potential

Figure 4.1 shows the convergence for the ground state eigenvalue  $e_{0n}$  and a spurious solution  $e_{1n}$  using  $\gamma = 1.01$ . After 14 iterations,  $e_{0n}$  quickly converged to

## 4.1 Dirac Equation for a Coulomb Potential

---

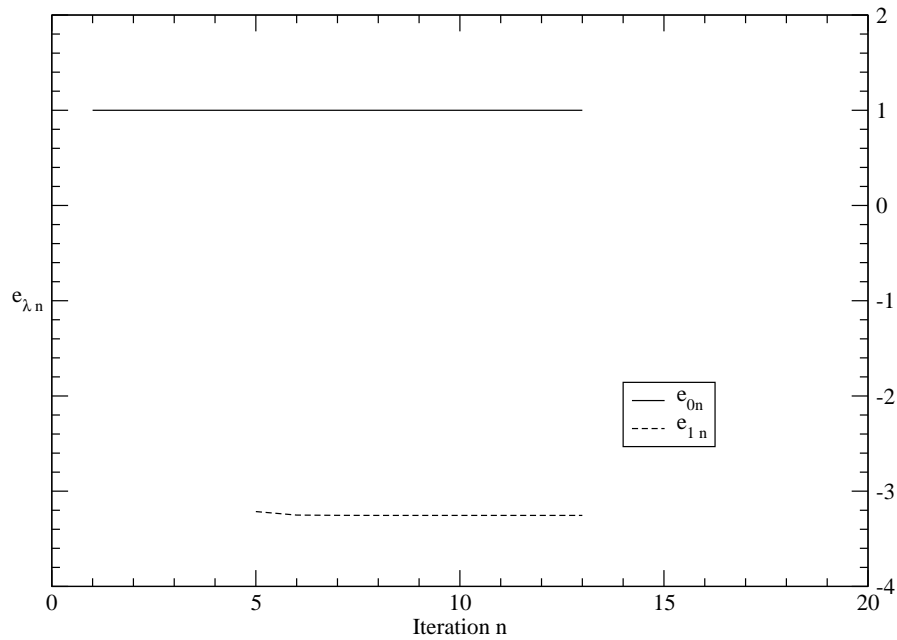


Figure 4.1: Plot of  $e_{\lambda n}$  convergence for Coulomb bound state and spurious solution for  $\gamma = 1.01$

## 4.1 Dirac Equation for a Coulomb Potential

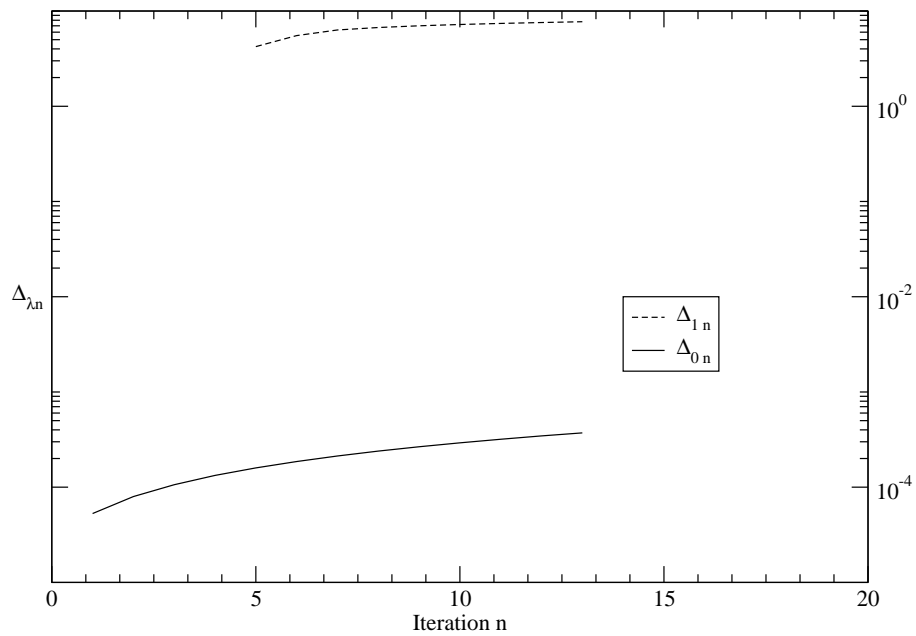


Figure 4.2: Plot of  $\Delta_{\lambda,n}$  convergence for Coulomb bound state and spurious solution for  $\gamma = 1.01$

## 4.2 Dirac Equation for a Yukawa Potential

---

the exact ground state value of  $E_o \simeq 0.999973374$  to 9 significant figures. The unphysical spurious solution converged to a value of  $-3.25419373$ .

Figure 4.2 shows the convergence of  $\Delta_{\lambda,n}$  for the ground state solution, and the spurious solution for  $\gamma = 1.01$ .  $\Delta_{\lambda,n}$  iteratively converges to zero for the bound state solution and converges to a non-zero value for the spurious solution.

## 4.2 Dirac Equation for a Yukawa Potential

In this case the potential was set to:

$$V(r) = -z\alpha \frac{\exp(-\lambda r)}{r} \quad (4.4)$$

The same slightly perturbed ground state solution derived by Bethe (Bethe (1964)) was used with ( $\kappa = -1$ ),  $z\alpha = 0.1$  and  $\lambda = 0.01$ .

### 4.2.1 Results: Yukawa Potential

Figure 4.3 shows the convergence for the ground state eigenvalue  $e_{on}$  and a spurious solution  $e_{1n}$  using  $\gamma = 1.01$ . After 10 iterations,  $e_{on}$  quickly converged to the exact ground state value of  $E_o \simeq 0.995917$ . This is to 6 decimal places of the value obtained by Krauthauser and Hill. The unphysical spurious solution converged to a value of  $-2.72280444$ .

Figure 4.4 shows the convergence of  $\Delta_{\lambda,n}$  for the ground state solution and the spurious solution for  $\gamma = 1.001$ .  $\Delta_{\lambda,n}$  iteratively converges to zero for the generated bound state solution and converges to a non-zero value for the spurious solution.

## 4.2 Dirac Equation for a Yukawa Potential

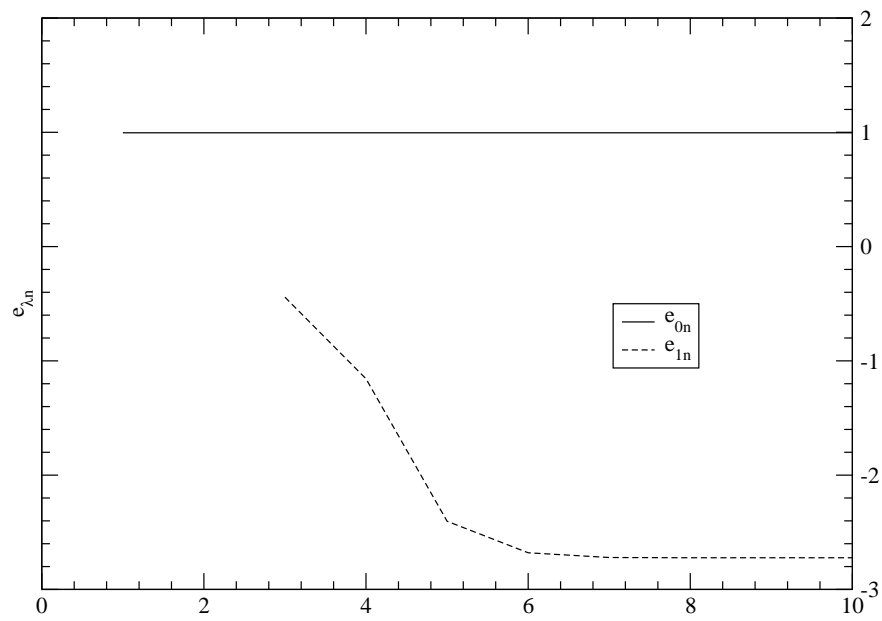


Figure 4.3: Plot of  $e_{\lambda n}$  convergence for Yukawa bound state and spurious solution for  $\gamma = 1.001$

## 4.2 Dirac Equation for a Yukawa Potential

---

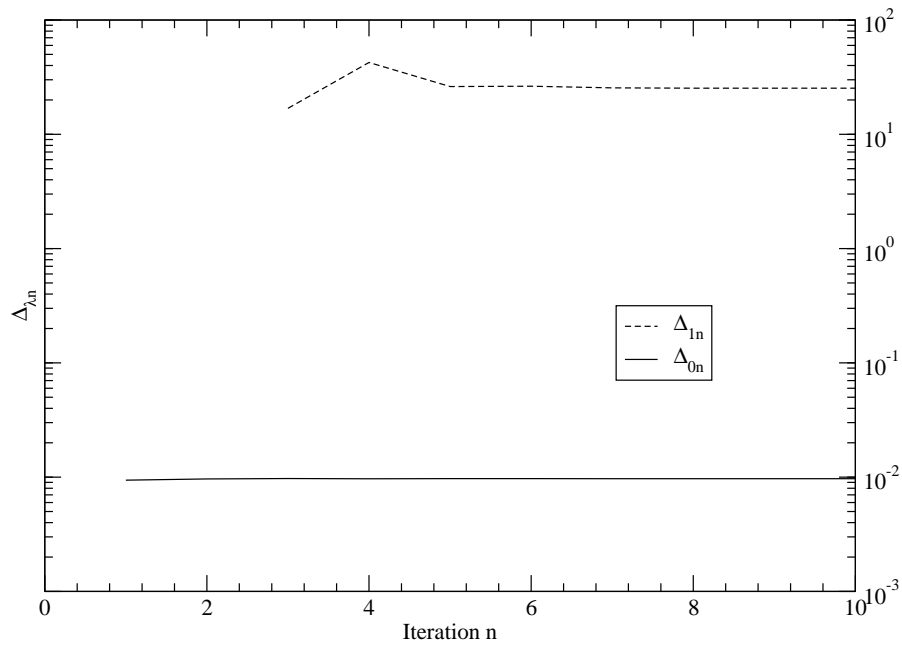


Figure 4.4: Plot of  $\Delta_{\lambda,n}$  convergence for Yukawa bound state and spurious solution for  $\gamma = 1.001$

# Chapter 5

## Conclusions

The main advantages of the Lanczos method over other methods to solve the Dirac problem are:

1. It can be applied to any self-adjoint operator which possesses at least one bound and is an absolutely convergent method.
2. The lowest-lying eigenpairs usually converge the quickest (Parlett (1980)), and one is able to obtain good approximations to the lowest-lying eigenpairs in this manner (especially the ground state).
3. The identification of the bound state solutions can easily be implemented.

In this dissertation, the Lanczos Algorithm has been used to obtain the ground state eigensolutions for the Coulomb and Yukawa potential Dirac Hamiltonians. In both cases, spurious solutions were successfully identified.

Since the Dirac problem contains point as well as continuous spectra, the bound states do not form a complete basis. Usually the start vector for the Lanczos algorithm is chosen from a complete set of analytic functions which define a space  $\mathcal{F}$ . This space is in most cases not necessarily of the same dimension as the subspace spanned by the exact eigenvectors. On the other hand, if the Lanczos algorithm is applied with this choice for the start vector, the eigenpairs obtained will correspond to those of the operator projected onto  $\mathcal{F}$ . A subset of these eigenstates must correspond to the exact eigenpairs of the unprojected Hamiltonian operator since the exact eigenstates can be expanded in terms of



the complete set of states which span  $\mathcal{F}$ . After each iteration, for each of the converging eigenpairs  $(e_{\lambda_n}, |e_{\lambda_n}\rangle)$ ,  $\Delta_{\lambda_n} = |e_{\lambda_n}^2 - \langle e_{\lambda_n} | \hat{H}^2 | e_{\lambda_n} \rangle|$  (where  $n$  is the iteration number) is calculated and a determination is made as to whether  $\Delta$  is converging toward zero or not. For the exact bound states of  $\hat{H}$ ,  $\Delta$  must be precisely zero, while the other eigenstates states of the projected operator should converge to some non-zero positive value. Provided sufficient iterations are performed, it is possible, in this manner to identify uniquely the approximate eigenpairs which ultimately will converge to the exact bound states. Since the genesis of these spurious states often occur in other solution methods for the Dirac problem based on the Rayleigh-Ritz method (such as the Finite basis-set and Fourier Grid methods), this method of bound state identification can also be applied.

## References

- E. Ackad and M. Horbatsch. *J. Phys. A*, 38:3157, 2005. 1, 2
- R. C. Andrew and H. G. Miller. *Phys. Lett. A*, 318:487, 2003. ii, 2, 3, 5, 8, 15
- R. C. Andrew, H. G. Miller, and G. D. Yen. *Solution of the Dirac Equation using the Lanczos Algorithm*. 2007. URL <http://www.citebase.org/abstract?id=oai:arXiv.org:0706.2236>.  
3
- R.C. Andrew and H.G. Miller. *A short note on the presence of spurious states in finite basis approximations*. 2007. URL <http://www.citebase.org/abstract?id=oai:arXiv.org:0711.3529>.  
ii, 1
- H. A. Bethe. *Intermediate Quantum Mechanics*. W. A. Benjamin, Inc., 1964. 16, 19, 22
- G. W. F. Drake and S. P. Goldman. *Phys. Rev. A*, 23:2093, 1981. 1
- S. P. Goldman. *Phys. Rev. A*, 31:3541, 1985. 1
- S. P. Goldman and G. W. F. Drake. *Phys. Rev. A*. 25:2877, 1982. 1, 2
- S. P. Goldman and G. W. F. Drake. *ADV. Atom. Mol. Phys.* 25:393, 1988. 1
- C. Krauthauser and R. Hill. *Can. J. Phys.*, 80:181, 2002. 1, 2
- K. G. Kreuzer, H. G. Miller, and W. A. Berger. *J. Phys. A*, 14:763, 1981a. 5, 6,  
7

## REFERENCES

---

- K. G. Kreuzer, H. G. Miller, and W. A. Berger. *Phys. Lett. A*, 81:429, 1981b. 15
- W. Kutzelnigg. *Int. J. Q. Chem.*, 25:107, 1984. 1
- C. Lanczos. *J. Res. Nat. Bur. Stand.*, 45:255, 1950. ii, 2, 5, 15
- H. G. Miller. *J. Math. Phys.*, 35:2229, 1994. 5, 9
- H. G. Miller and W. A. Berger. *J. Phys. A*, 12:1693, 1979. 14
- A. Mostafazadeh. *J. Math. Phys.*, 42:3372, 2001. 9, 11
- B. N. Parlett. *The Symmetric Eigenvalue Problem*. Prentice Hall, Englewood Cliffs, N. J., 1980. ii, 3, 8, 14, 25
- B. Thaller. *The Dirac Equation*. Springer, New York, 1992. 15
- K. Willner, O. Dulieu, and F. Masnou-Seeuws. *J. Chem. Phys.*, 120:548, 2004. 2
- S. Wolfram. *Mathematica A System for Doing Mathematics by Computer - second edition*. Addison-Wesley, Redwood, California, 1991. 7